Engineering Analysis with Boundary Elements 33 (2009) 1348–1361

Contents lists available at ScienceDirect

Engineering Analysis with Boundary Elements

journal homepage: www.elsevier.com/locate/enganabound

On the choice of source points in the method of fundamental solutions

Carlos J.S. Alves

Departamento de Matemática & CEMAT, Instituto Superior Técnico, T.U. Lisbon, Portugal

ARTICLE INFO

Article history:
Received 18 March 2009
Accepted 2 May 2009
This paper is dedicated to the memory of Michael Golberg.
Available online 24 July 2009

Keywords:
Method of fundamental solutions
Boundary integral equations
Partial differential equations
Meshfree methods
Radial basis functions

ABSTRACT

The method of fundamental solutions (MFS) may be seen as one of the simplest methods for solving boundary value problems for some linear partial differential equations (PDEs). It is a meshfree method that may present remarkable results with a small computational effort. The meshfree feature is particularly attractive when we need to change the shape of the domain, which occurs, for instance, in shape optimization and inverse problems. The MFS may be viewed as a Trefftz method, where the approximations have the advantage of verifying the linear PDE, and therefore we may bound the inner error from the boundary error, in well-posed problems. A main counterpart for these global numerical methods, that avoid meshes, are the associated linear systems with dense and ill conditioned matrices. In these methods a sort of uncertainty principle occurs—*we cannot get both accurate results and good conditioning*—one of the two is lost. A specific feature of the MFS is some freedom in choosing the source points. This might lead to excellent results, but it may also lead to poor results, or even to impossible approximations. In this work we will discuss the choice of source points and propose a choice along the discrete normal direction (following [Alves CJS, Antunes PRS. The method of fundamental solutions applied to the calculation of eigenfrequencies and eigenmodes of 2D simply connected shapes. Comput Mater Continua 2005;2(4):251–66]), with a possible local criterion to define the distance to the boundary. We will also address some extensions that connect the asymptotic MFS to other methods by choosing the sources on a circle/sphere far from the boundary. We also present a direct connection between the approximation based on radial basis functions (RBF) and the MFS approximation in a higher dimension. This increase in dimension was somehow already present in a previous work [Alves CJS, Chen CS. A new method of fundamental solutions applied to non-homogeneous elliptic problems. Adv Comput Math 2005;23:125–42], where the frequency was used as the extra dimension. The free parameters in RBF inverse multiquadrics 2D approximation correspond in fact to the source point distance to the boundary plane in a Laplace 3D setting. Some numerical simulations are presented to illustrate theoretical issues.

1. Introduction

In 1998, while deducing some density results with fundamental solutions, for near field inverse problems, I realized that this lead to a numerical method for solving PDEs. Later on, when I met C.S. Chen at the BEM XXI (1999) conference, it was clear that this method was the method of fundamental solutions (MFS), an established but misregarded method for solving PDEs. One of the most influential researchers that was struggling for the MFS recognition was clearly Michael Golberg. It was Michael that told me the short history of the MFS in an unforgettable car trip with C.S. Chen from LV to LA, to attend the ICCES 2000 conference. Michael liked to emphasize two points in favor of the MFS—its simplicity together with the exponential rate of convergence. In fact, he even considered to establish a competition to prove that no other method could perform better, in terms of implementation time and precision results, at least for the Laplace equation. On the other hand, he was concerned with the lack of mathematical justification for the convergence results together with ill conditioning and with the uncertainty in the location of the point-sources. I would like to dedicate this paper to Michael's memory, and contribute by clarifying some results concerning the performance of the MFS, mainly with respect to the location of the source points, and also to present some extensions.

The MFS is a global numerical method, included in the broad class of methods using particular solutions, also known as Trefftz methods. It may also be included in the class of spectral methods, as it presents exponential rate of convergence, under some regularity assumptions. The MFS was introduced in the 1960s by Kupradze and Aleksidze in [30] (see also [13], Oliveira implemented it to avoid singular integration in the boundary element method, BEM). It has been readdressed several times in 1970s and 1980s (see e.g. [20,22]). In the context of meshfree methods the

E-mail address: calves@math.ist.utl.pt

0955-7997/$ - see front matter © 2009 Elsevier Ltd. All rights reserved.
doi:10.1016/j.enganabound.2009.05.007

MFS gained more attention in recent years, being used for several applied problems.

Outline of the text: We start by extending this introduction presenting a brief and general framework in Section 2. We will consider both interior and exterior problems, since the application to exterior problems is one advantage of the MFS shared with the BEM. The underlying justifications are basically the same, and we may address both cases with the same framework. In Section 3 we start by presenting the classical MFS, and discuss admissible choices for source points in terms of density and linear independence results. We also discuss the interpolation and least squares approaches, the ill conditioning vs. accuracy paradigm and propose a choice for source points based on the normal algorithm and a *glocal* technique. In Section 4 we consider some extensions, starting by emphasizing that we may consider other choices for fundamental solutions that incorporate an enrichment, and we recall that the asymptotic behavior of the MFS may be related to other methods, such as the plane waves method. We consider the MFS not only for boundary approximation but also for domain approximation—either by adding frequency as an extra dimension or simply to consider the domain as a boundary in a higher dimensional space—then related to standard RBF approximations. Finally, in Section 5 we present some numerical simulations to illustrate some chosen issues presented in the previous sections.

2. General setting

2.1. Interior and exterior settings

Consider a boundary value problem for a bounded domain $\Omega \subset \mathbb{R}^d$, with regular (at least piecewise C^1) boundary $\Gamma = \partial\Omega$. We denote by $\mathscr{A}$ a second order differential operator, linear and elliptic, and consider $\mathscr{B}$ to be a boundary operator.

Interior setting: In a general framework given the data functions f and g, we search for a solution u such that

$$\begin{cases} \mathscr{A}u = f & \text{in } \Omega, \\ \mathscr{B}u = g & \text{on } \Gamma. \end{cases} \tag{1}$$

In this interior setting we also consider the non-simply connected case. This means that Ω or its exterior $\mathbb{R}^d\backslash\overline{\Omega}$ may have more than one connected component.

Exterior setting: For exterior problems we assume the domain to be $\mathbb{R}^d\backslash\overline{\Omega}$ and an extra asymptotic condition is needed,

$$\begin{cases} \mathscr{A}u = 0 & \text{in } \mathbb{R}^d\backslash\overline{\Omega}, \\ \mathscr{B}u = g & \text{on } \Gamma, \\ (\mathscr{B}_\infty u)(x) = o(r^p) & \text{when } r = |x| \to \infty. \end{cases} \tag{2}$$

The last condition in (2) restricts the asymptotic behavior of the solution, by posing a condition at the "infinite boundary", and it is usually considered in radial terms, uniformly for all directions.

For instance, consider the exterior Helmholtz equation, with $\mathscr{A} = -(\Delta + \kappa^2)$. Here κ is the constant wavenumber (or the frequency, for unitary wave propagation speed). The acoustic asymptotic behavior of the wave amplitude u is given by the Sommerfeld radiation condition $\mathscr{B}_\infty u = \partial_r u \pm i\kappa u$ (the sign is plus for incoming waves and minus for outgoing waves, the latter being the one with physical meaning from the time-dependent problem). The decreasing rate must be uniform for all directions, and depends on the dimension, with $p = (1-d)/2$. In the wave propagation problem, that we will be interested in, this asymptotic behavior allows to define a far-field pattern u_∞ that characterizes the wave at infinity, for instance, for 3D acoustic waves,

$$u(x) = \frac{e^{i\kappa r}}{r}(u_\infty(\hat{x}) + O(r^{-1})) \quad \text{when } r = |x| \to \infty \tag{3}$$

with $\hat{x} = x/r$. This asymptotic behavior will be useful in analyzing the asymptotic method of fundamental solutions, later on.

2.2. Fundamental solutions

Given a linear differential operator $\mathscr{A}$, a fundamental solution Φ verifies in the distribution sense,

$$\mathscr{A}\Phi = \delta \quad \text{meaning} \langle \mathscr{A}\Phi, \varphi \rangle = \varphi(0), \ \ \forall \varphi \in \mathscr{D}(\mathbb{R}^d) \tag{4}$$

with $\mathscr{D}(\mathbb{R}^d) = \{\varphi \in C^\infty(\mathbb{R}^d) : \text{supp}(\varphi) \subset \mathbb{R}^d\}$, the space of test functions in distribution theory. Here δ stands for the Dirac delta distribution centered at the origin, and the expression has meaning in $\mathscr{D}'(\mathbb{R}^d)$, the distribution dual space.

From the Ehrenpreis–Malgrange (1954, 1955) theorem, we know that for constant coefficient differential operators $\mathscr{A}$ there exist fundamental solutions Φ in the distribution sense that may have an explicit form (e.g. [23]).

Theorem 1 (*Ehrenpreis, Malgrange*). *Let $\mathscr{A} = p(\partial)$, with p a non-null polynomial with variables in the partial differential vector $\partial = (\partial_1, \ldots, \partial_d)$, then there exists a distribution $\Phi \in \mathscr{D}'(\mathbb{R}^d)$:*

$$\langle p(\partial)\Phi, \varphi \rangle = \varphi(0), \quad \forall \varphi \in \mathscr{D}(\mathbb{R}^d).$$

Remark 1.1. Note that in vectorial PDEs the fundamental solutions are tensors, and then δ stands for a vector with Dirac delta components.

Remark 1.2. The fundamental solution *is not unique*: it is clear that given any entire solution $\mathscr{A}w = 0$ in $\mathbb{R}^d$, then $\Phi + w$ will also be a fundamental solution. When real differential operators lead to complex fundamental solutions (for instance, the Helmholtz operator) then the conjugate is a fundamental solution and therefore we also have a family of fundamental solutions $\{\alpha\Phi + (1-\alpha)\overline{\Phi} : \alpha \in [0,1]\}$. A main difference between fundamental solutions is their asymptotic behavior, which is especially important for exterior problems.

2.2.1. Explicit fundamental solutions

Although not unique, the notion of fundamental solution is usually associated with a certain and known explicit form.

Just as examples for possible applications of the following theory, we present some fundamental solutions associated with some operators.

For instance, when $\mathscr{A} = -\Delta$ (Laplacian), we get simple expressions ($x \neq 0$)

$$\Phi(x) = \frac{-1}{2\pi}\log|x| \ \text{ when } d = 2, \quad \Phi(x) = \frac{1}{4\pi|x|} \ \text{ when } d = 3 \tag{5}$$

and also for the Helmholtz operator, $\mathscr{A} = -(\Delta + \kappa^2)$, explicit expressions are

$$\Phi(x) = \frac{i}{4}H_0^{(1)}(\kappa|x|) \ \text{ when } d = 2, \quad \Phi(x) = \frac{e^{i\kappa|x|}}{4\pi|x|} \ \text{ when } d = 3, \tag{6}$$

where $H_0^{(1)}$ stands for the first kind Hankel function, defined by the Bessel functions J_0 and Y_0, the latter presenting a logarithmic-like singularity. Both these fundamental solutions inherit from the Laplace operator a radial feature that is not present in some other operators, for instance in some well-known vectorial differential operators.

In the vectorial case, the fundamental solution $\mathbf{\Phi}$ is a tensor, for example when $\mathscr{A} = -\nabla \cdot \sigma$ is the Lamé operator (σ being the stress tensor) the fundamental solution is then given by

$$\Phi_{ij}(x) = \begin{cases} \dfrac{\lambda+3\mu}{4\pi\mu(\lambda+2\mu)}\left(-\log|x|\delta_{ij} + \dfrac{\lambda+\mu}{\lambda+3\mu}\dfrac{x_i x_j}{|x|^2}\right) & \text{when } d=2, \\ \dfrac{\lambda+3\mu}{8\pi\mu(\lambda+2\mu)}\left(\dfrac{1}{|x|}\delta_{ij} + \dfrac{\lambda+\mu}{\lambda+3\mu}\dfrac{x_i x_j}{|x|^3}\right) & \text{when } d=3. \end{cases} \tag{7}$$

All these fundamental solutions are analytic functions—except at the origin, where they are singular.

This singularity may be shifted, and this leads to the definition of a point-source that is in the basis of the method of fundamental solutions (MFS) and the boundary element method (BEM).

Definition 1 (*Source set*). Given a source point $z \in \mathbb{R}^d$, a *point-source* (or point-force) $\Phi_z = \Phi(\cdot - z)$ is a shifted fundamental solution, thus verifying $\mathscr{A}\Phi_z = \delta_z = \delta(\cdot - z)$. When considering source points $z \in \omega$ on some set ω, we call *source set* to ω.

The notion of a point-source, although trivial, will be important in the following. In the MFS the source set is external to the domain, while in the BEM it coincides with the boundary.

A convolution with a fundamental solution can be associated with a Huygens principle. Each point will act like a source, and the whole contribution will be integrated, weighted by a density function.

Theorem 2. *Let Φ be a fundamental solution of $\mathscr{A} = p(\partial)$. Then the convolution $u = \Phi * f$ (when defined) is a particular solution of $\mathscr{A}u = f$.*

Proof. This result can be seen as an obvious consequence of convolution properties for derivatives (and the Dirac delta is the convolution neutral element)

$$\mathscr{A}u = p(\partial)(\Phi * f) = (p(\partial)\Phi) * f = \delta * f = f. \qquad \square$$

2.3. Newtonian and layer potentials

The convolution property in Theorem 2 leads to the representation in potential theory (e.g. [16]). Taking an extension by zero outside a domain ω, say $f = \chi_\omega \phi$ (here χ_ω stands for the characteristic function of ω), we have $u = \Phi * f$ and the Newtonian potential

$$u(x) = (\mathscr{N}\phi)(x) = \int_\omega \Phi(x-y)\phi(y)\,dy. \tag{8}$$

Here the source set is the whole domain ω.

The convolution can also be used to obtain single and double layer potentials, when f is considered to be a boundary distribution. Let γ be a regular orientable $d-1$ manifold, then $f = \alpha\delta_\gamma$ leads to the single layer potential

$$u(x) = (\mathscr{L}\alpha)(x) = \int_\gamma \Phi(x-y)\alpha(y)\,dy \tag{9}$$

and taking $f = \partial_{\mathbf{n}}(\beta\delta_\gamma)$, where $\partial_{\mathbf{n}}$ denotes the normal derivative, we obtain the double layer potential

$$u(x) = (\mathscr{M}\beta)(x) = \int_\gamma \partial_{\mathbf{n}(y)}\Phi(x-y)\beta(y)\,dy. \tag{10}$$

In both these cases the source set is γ.

Remark 2.1. Note that in the vectorial setting the normal derivative is to be taken in the appropriate sense, and $\partial_{\mathbf{n}(y)}\Phi$ will be a three-indexed tensor. The discussion here is restricted to second order PDEs, but it may be adapted to higher order operators, such as the bilaplacian $\mathscr{A} = \Delta^2$, considering triple and quadruple layer potentials (defined with the Laplacian trace and normal derivative of the Laplacian). We do not consider here time-dependent problems, where the fundamental solutions are only analytic in the half-space ($t > 0$).

Remark 2.2. When the fundamental solutions are analytic everywhere except at the origin, this means that these potentials define analytic functions outside γ (or ω) that will also be particular solutions of the homogeneous differential equation $\mathscr{A}u = 0$. In the cases of single or double layer potentials, choosing a normal direction $\mathbf{n}$, we consider two traces, one following $\mathbf{n}$ and the other following $-\mathbf{n}$. The single and double layer potentials present jumps defined by the densities. The single layer operator $\mathscr{L}$ presents a normal derivative jump defined by α, and the double layer operator $\mathscr{M}$ presents a jump defined by β. The layer potentials are analytic everywhere except at the boundary γ.

2.4. BIEM and MFS

One possible interpretation of the method of fundamental solutions is to relate it to boundary integral equation methods (BIEM), like the boundary element method, considering the discretization of the single layer potential

$$u(x) = (\mathscr{L}_\gamma\alpha)(x) = \int_\gamma \alpha(y)\Phi(x-y)\,dy \approx \tilde{u}(x) = \sum_k \alpha_k \Phi(x-y_k).$$

This is meaningful whenever we take quadrature nodes y_k on a boundary γ and the corresponding weights w_k are incorporated in the unknown coefficients $\alpha_k = \alpha(y_k)w_k$ (together with the unknown density function evaluated at the nodal points). In both cases, since $\mathscr{L}_\gamma\alpha$ (or $\mathscr{M}_\gamma\beta$, in the case of double layer formulation) verifies the equation inside Ω, we only need to fit the boundary condition (for instance, in the Dirichlet case, $\tilde{u} = g$, with an appropriate density).

Both methods relate to point-sources and layer potentials, however we should take into account the following remarks:

(i) Unlike the BIEM, in the MFS we do not take $\gamma = \partial\Omega$, i.e. the source set does not coincide with the boundary. In the MFS, the source set $\gamma \subset \mathbb{R}^d \backslash \overline{\Omega}$ is artificial, and we avoid singular integrations, at the cost of having higher ill conditioning problems.

(ii) In the BIEM we may use double layer representation in Dirichlet problems (or single layer in Neumann problems) to avoid ill conditioning, but in the MFS this strategy does not avoid ill conditioning problems. Moreover, for regular data, the results get better for artificial boundaries far from the true boundaries, where the conditioning is worse.

(iii) In the MFS, while taking $u = \mathscr{L}_\gamma\alpha = g$ on $\partial\Omega$, with external $\gamma \subset \mathbb{R}^d \backslash \overline{\Omega}$, this can only have a solution for analytic g. In fact, any convolution with the analytic fundamental solution Φ is analytic except at γ and therefore the MFS only provides a sequence of analytic approximations to g. There is no hope in solving the BIE $\mathscr{L}_\gamma\alpha = g$ in a single stage, for non-analytic g.

Thus, we emphasize that the relation between the MFS and the BIEM is rather a theoretical tool than a direct connection.

(iv) In the MFS the choice for the source set is quite arbitrary. These lead (almost) always to linearly independent particular solutions, and in the sense of a Trefftz method we may add as many source points as we which. The price to pay in doing this in a random fashion is that the approximation does not improve much, and it can even get worse, because the ill conditioning will increase rapidly.

In the following we discuss some possibilities for source sets, and we will see that only some of them lead to an effective numerical method.

3. Classical MFS

As mentioned in the introduction, the method of fundamental solutions, also known as charge simulation method, was introduced in 1964, by Kupradze and Aleksidze [30]. In [13] Oliveira used it to avoid singularities of the boundary integral equation of the first kind, and later Mathon and Johnston [32] set it as an independent numerical method. Considering enclosing circles as artificial boundaries, Bogomolny [15] established some density results in Sobolev spaces for Laplace problems, and presented an exponential convergence result. Clarifying some assumptions, this exponential rate of convergence for Laplace 2D problems, was also analyzed by Katsurada [26] (in the context of complex analysis). A good account of the early developments of the MFS can still be found in the review paper by Fairweather and Karageorghis [20] (see also [21], for scattering problems).

The classical MFS using a source set γ may be resumed in the following steps:

(I—*setting the points*): Define some collocation points on the boundary $x_1,\dots,x_n \in \partial\Omega$, and the external source points $y_1,\dots,y_m \in \gamma$ (usually with $n \geq m$, see the three scenarios in [37]) and the corresponding point-source approximations

$$v_m(x) = \sum_{j=1}^{m} \Phi_{y_j}(x)\alpha_j, \tag{11}$$

which are particular solutions to $\mathscr{A}v_m = 0$. For completeness, or accuracy purposes, an enrichment with extra basis functions might be needed (e.g. in Laplace 2D problems, a constant function is needed).

(II—*solving the system*): Impose the boundary conditions $\mathscr{B}v = g$, at the given collocation points

$$\sum_{j=1}^{m} \mathscr{B}\Phi_{y_j}(x_i)\alpha_j = g(x_i) \quad (i = 1,\dots,n) \tag{12}$$

and find the coefficients α_j such that (12) is verified—either in the interpolation sense ($n = m$ case), or in the least squares sense ($n \geq m$ case), with or without regularization.

In scalar problems, if $\mathbf{M}$ is the matrix defined by the entries $M_{ij} = \mathscr{B}\Phi_{y_j}(x_i)$,

$\mathbf{a}$ the vector defined by the coefficients α_j, and $\mathbf{g}$ the vector defined by $g(x_i)$, then:

- in the interpolation sense, we may obtain the coefficients by solving a linear system $\mathbf{Ma} = \mathbf{g}$,
- and in the least squares sense, by solving $\mathbf{M}^*\mathbf{Ma} = \mathbf{M}^*\mathbf{g}$.

Since these systems in general are ill conditioned, a simple way to circumvent machine precision difficulties is to consider a Tikhonov regularization procedure with a very small parameter $\tau > 0$, and solve

$$(\tau\mathbf{I} + \mathbf{M}^*\mathbf{M})\mathbf{a} = \mathbf{M}^*\mathbf{g}. \tag{13}$$

The choice of the parameter τ can be controlled by the Morozov discrepancy principle (e.g. [17,28]).

(III—*checking the approximation*): Let $\alpha_j^{(n)}$ be the coefficients calculated in (II). The approximating solution is

$$v_{m,n}(x) = \sum_{j=1}^{m} \Phi_{y_j}(x)\alpha_j^{(n)} \tag{14}$$

satisfying $\mathscr{A}v_{m,n} = 0$ on Ω and approximating the boundary condition.

As, in general, there are no convergence results, the MFS is only an *a posteriori* method, and $v_{m,n}$ can only be regarded as an approximation if we check the boundary data.

The well posedness of problem (1) implies that the boundary error

$$E_{m,n} = g - \mathscr{B}v_{m,n} \quad \text{on } \partial\Omega, \tag{15}$$

defines the quality of the approximation (for instance, by the maximum principle in Laplace problems, we know that the internal error will be smaller than the error on the boundary approximation).

In general we may rely on the *a posteriori error estimate*:

$$\|u - v_{m,n}\|_{\Omega} \leq C\|g - \mathscr{B}v_{m,n}\|_{\partial\Omega},$$

for some theoretical constant $C > 0$ in the appropriate Sobolev (or Hölder) norms, using the well posedness of the direct problem (for the Laplace equation we may use the maximum norm).

Note that, in discrete terms, it is not enough to check the boundary approximation at the collocation points. Other, different boundary points, must also be used. Also, depending on the boundary norm, tangential derivatives might be needed to evaluate the quality of the boundary approximation. For instance, in the Helmholtz case, one should check the $H^{1/2}(\partial\Omega)$ boundary norm, and it would be enough to check the function together with the tangential derivative in terms of the stronger $H^1(\partial\Omega)$ norm.

Therefore, the MFS is one of the simplest PDE numerical methods to implement and it provides remarkable results for some standard data (regular boundaries and boundary conditions). Unlike other classical methods, we can obtain almost machine precision accuracy with small matrices and no meshing procedure. Thus, there is no point in requiring further precision from the MFS, as it is at a level of precision far better than the possible improvements that classical mesh based methods allow for themselves.

Also the MFS is reliable as it allows to control the error by direct inspection of the boundary approximation—this fact, depicted in step (III), is usually misregarded.

The meshfree feature, together with easy implementation and some excellent results, saves time in the implementation and testing of different models for different problems in applications. This attracted engineering researchers to the MFS in recent years.

However, as expected, there is a counterpart. As the boundary element method, the MFS is restricted to some PDEs, while needing a fundamental solution, and it was also restricted to homogeneous problems ($f = 0$). On the other hand, unlike classic meshing methods, MFS and BEM are particularly suited for exterior problems, as they do not require the construction of an artificial boundary to bound the numerical domain. Also, there are techniques to both BEM and MFS that allow to solve other PDE problems, linear or non-linear, for instance by iterative procedures. Both methods reduce the dimension of the linear system, but while the BEM presents singular integration difficulties, the MFS presents ill conditioning difficulties. An advantage of the MFS (over BEM) is that it also avoids a boundary mesh, especially important for 3D problems.

The ill conditioning feature of the MFS strongly depends on the choice of source points. The singularity of the fundamental solution means that choosing source points very close to the boundary collocation points leads to big diagonal entries, and in the limit, to a diagonally dominant matrix. However, this means that we are almost in a BEM choice, without singular integration. In that case the ill conditioning problems disappear but, while ignoring the singular integration, MFS performs poorly.

3.1. Choosing the source points

From early density results and some exponential convergence results with increasing radius, one of the most common choices is to place the source points on a circle (or sphere, in 3D) far from the boundary. Far, but not too far, otherwise severe machine precision problems will occur due to ill conditioning (early results with single precision would be discouraging). On the other hand, considering the MFS as BEM variant, the points should follow the boundary, but not too close, since this will lead to better conditioning but worse accuracy.

These are far from being the only possibilities, and some researchers prefer to consider random centers for point-sources. In fact, any point-source with an external center will be a particular solution, and therefore there is a certain amount of freedom in choosing the source points. However, we also remark that arbitrary choices for source points might lead to impossible or poor approximations.

3.1.1. Incomplete source sets

We present two situations for source sets that lead to impossible approximations with the MFS.

(i) If the fundamental solution has a radial feature, meaning $\Phi(x)=\phi(|x|)$, then a symmetry property will occur

$$\forall_{j=1,\dots,m}|x-y_j|=|x^*-y_j|\Rightarrow v_m(x)=\sum_{j=1}^{m}\Phi(x-y_j)\alpha_j=\sum_{j=1}^{m}\Phi(x^*-y_j)\alpha_j=v_m(x^*).$$

This happens for instance if we consider collinear (coplanar, in 3D) source points. For instance in 2D, if $y_{j,1}=0$ then with $x^*=(-x_1,x_2)$ we have the symmetry property $v_m(x)=v_m(x^*)$. Therefore, if the line (or plane, in 3D) cuts the boundary, then the solution must verify the same property (symmetry over the x axis). If the solution u does not verify $u(x)=u(x^*)$, for some $x,x^*\in\partial\Omega$, this choice of points will lead to an impossible approximation v.

- Likewise, if we consider collocation points on a line (or a plane), source points with the same projection point will produce the same values, leading to linear dependence, and non-invertible matrices.

More precisely, it is clear that, for instance, given the source points y and $y^*=(-y_1,y_2)$ we have $\Phi(x-y)=\Phi(x-y^*)$ for all $x:x_1=0$.

(ii) Suppose that, besides the radial feature, the fundamental solution also vanishes at some distance, that is $\phi(r)=0$, for some $r>0$. Then, if we choose source points on a circle verifying $|y_j-c|=r$, then the approximation value in the center is null, $v_m(c)=\sum\phi(|c-y_j|)\alpha_j=0$. Therefore, solutions not null at that center point $c\in\Omega$ cannot be approximated.

- This occurs with the 2D Laplace fundamental solution because $\log(1)=0$, giving impossible approximations for some circles when the solution is not null at that center (or if we do not add an extra constant basis function).
- This occurs if we just take the imaginary or real part of the Helmholtz fundamental solution (in 2D or 3D).

If we consider only $J_0(\kappa|x-y|)$ (or $Y_0(\kappa|x-y|)$) instead of the full $H_0^{(1)}(\kappa|x-y|)$ the vanishing problem will clearly occur for circular source sets when the wavenumber times the radius equals a zero of the Bessel functions.

(iii) Suppose that the domain is doubly connected, for instance an annulus $\Omega=B(0,r)\backslash\overline{B}(0,1)$ with $r>1$. If one takes Dirichlet data to verify $g(x)=0$ for $|x|=1$, and $g(x)=1$ for $|x|=r$, then it is impossible to approximate these Dirichlet data using only source points $|y|>r$ (no matter where). By imposing $g=0$ on $|x|=1$ and as the approximation $\tilde{u}$ verifies the equation in $|x|<1$ this implies $\tilde{u}=0$ on the open set, and since $\tilde{u}(x)$ is analytic for $|x|<r$ it is null and this proves to be impossible to verify also $g=1$ on $|x|=r$.

This example shows that in the case of multiply connected sets, we have to place source points in all connected components of the exterior domain.

3.1.2. Exceptional source sets in Laplace equation

As a counterpart, there are cases where it is possible to find remarkably good approximations, and in some cases the data produced by internal sources may be reproduced exactly by external source points.

(i) An exceptional situation occurs for the Laplace equation, considering the Green–Dirichlet function for an unitary circle/sphere, $\Omega=B(0,1)$.

Let $|y|>1$ and take $y^*=y/|y|^2\in B(0,1)$, then

$$G_y(x)=\Phi(x-y)-\Phi(|y|(x-y^*)) \tag{16}$$

verifies $G_y=0$ on $\partial\Omega$. The boundary data $g(x)=\Phi(|y|(x-y^*))$ is reproduced by taking $u(x)=\Phi(x-y)$, that verifies both the (Laplace) equation and the (Dirichlet) boundary condition.

In this case, a single external source placed exactly on $y^*\in\mathbb{R}^d\backslash\overline{\Omega}$ performs the whole approximation.

The same thing happens if we take linear combinations, for instance assume that

$$g(x)=\sum_k\alpha_k\Phi(|y_k|(x-y_k^*))$$

then $u(x)=\sum_k\alpha_k\Phi(x-y_k)$ is the exact solution to the Laplace equation.

This situation is exceptional for the disk problem in Laplace equation, but also allows to understand the relation between the approximation for the interior and the exterior problems, since the roles may be inverted.

(ii) Another quite favorable situation in the Laplace 2D equation is given with the help of complex analysis and conformal mapping. As proven by Katsurada [26] this may lead to exponential convergence rate, when both the boundary $\partial\Omega$ and the Dirichlet data g are analytic if we are able to map the circle into the analytical boundary $\partial\Omega$.

3.1.3. Density, linear independence and a posteriori error

From these previous considerations we see that the choices for source sets might lead, in some cases, to impossible approximations, but in other cases they may also lead to excellent approximations, or even to exact solutions. Beside the 2D analytical situation for the Laplace equation ([26], see also [14] for the Helmholtz case), analyzed in the context of complex analysis, the lack of *a priori* convergence results in a general framework, puts the choice of the source set for the MFS in terms of *a posteriori* results.

A main challenge in the MFS is to choose the source points so that a good approximation is possible from a small number of point-source functions. This is also a balance between two things. On one hand, for completeness purposes, we need more source points to improve the approximations, while on the other hand, adding source points leads to linear independence problems, meaning worse conditioning.

We now present some results concerning linear independence and density. As long as these results are proven we can test the approximation with the admissible source sets and check the

quality of the approximation with the a posteriori error estimate as mentioned in the MFS step (III).

3.2. Density results

In terms of density, we want to find source sets γ such that the MFS function space

$$\mathscr{G}_\gamma = \text{span}\{\Phi_y|_{\partial\Omega} : y \in \gamma\} \tag{17}$$

is dense in a functional space defined on $\partial\Omega$. Density proofs for $L^2(\partial\Omega)$ can be easily adapted to appropriate Sobolev spaces, substituting the L^2 inner product by duality (see e.g. [15,9], see also [35] for a Hölder setting). Bogomolny [15] relates the MFS to the BEM, and considers the MFS as discrete versions of the approximations, using single layer boundary potentials on γ,

$$(\mathscr{L}_\gamma\alpha)(x) = \int_\gamma \Phi(x-y)\alpha(y)\,dy. \tag{18}$$

Unlike that approach, by proving density with the span $\mathscr{G}_\gamma$ we are only considering the MFS to be finite sums on a set γ, that also might be an open set ω (in that case, the notation $\mathscr{N}_\omega\alpha$ would then be more appropriate).

In the following we assume that problem (1) is well posed in Ω and that we are considering the fundamental solutions Φ analytic (except at the origin), which is the common case for constant coefficient second order elliptic operators $\mathscr{A}$. Then from the properties of boundary layer potentials, we present the following result using the definition of the *external source set condition*.

Definition 2. We say that a source set $\gamma \subset \mathbb{R}^d\backslash\overline{\Omega}$ verifies the *external source set condition* if for any function w verifying $\mathscr{A}w = 0$ in $\mathbb{R}^d\backslash\overline{\Omega}$ we have the uniqueness property

$$\forall x \in \gamma,\ w(x) = 0 \Longrightarrow \forall x \in \mathbb{R}^d\backslash\overline{\Omega},\ w(x) = 0.$$

Theorem 3. *Assume that $\gamma \subset \mathbb{R}^d\backslash\overline{\Omega}$ verifies the external source set condition. Consider $\mathscr{L}_{\partial\Omega}$ a continuous single layer boundary potential defined on a Sobolev boundary space $H^{-r}(\partial\Omega)$. If* $\text{Ker}(\mathscr{L}_{\partial\Omega}) = \{0\}$, *then the MFS function space $\mathscr{G}_\gamma$ is dense in the dual space $H^r(\partial\Omega)$.*

Proof. Define, by duality,

$$w(y) = (\mathscr{L}_{\partial\Omega}\alpha)(y) = \langle \Phi_y, \alpha\rangle_{\partial\Omega}$$

which is an analytic function outside $\partial\Omega$, continuous through that boundary (from the properties of single layer potentials for second order elliptic problems, usually $\alpha \in H^{-1/2}(\partial\Omega)$ is the normal derivative jump).

We want to prove that $\langle \Phi_y, \alpha\rangle = 0$, for all $y \in \omega$, implies $\alpha = 0$.

By definition, γ verifies the external source set condition and since $\mathscr{A}w = 0$ in $\mathbb{R}^d\backslash\overline{\Omega}$ we have $w = 0$ in $\mathbb{R}^d\backslash\overline{\Omega}$.

This means that the external trace w^+ is null, and the continuity through the boundary implies $w^- = 0$. Since $\mathscr{A}w = 0$ in Ω, and $w = 0$ on $\partial\Omega$, the well posedness of (1) (or (2), for the exterior problem) implies $w = 0$ in Ω, and therefore $w = 0$ in $\mathbb{R}^d\backslash\partial\Omega$. This means $\alpha = 0$, because $\text{Ker}(\mathscr{L}_{\partial\Omega}) = 0$. Let τ_γ be the operator that defines the trace (or restriction) to γ. We have proven that $\text{Ker}(\tau_\gamma\mathscr{L}_{\partial\Omega}) = \{0\}$. Thus $\mathscr{G}_\gamma$ defined by the range of $\tau_{\partial\Omega}\mathscr{L}_\gamma$, the adjoint of $\tau_\gamma\mathscr{L}_{\partial\Omega}$, is dense (by the Hahn-Banach theorem) in the dual space $H^r(\partial\Omega)$. □

Remark 3.1. The proof is sufficiently general and it even includes non-simply connected or exterior domains. Similar and more appropriate results could be derived for boundary conditions other than Dirichlet.

Remark 3.2. We did not specify the Sobolev spaces used, but for instance for Laplace or Helmholtz operators we may take $r \le 1/2$ and usually the density is proven in $H^{1/2}(\partial\Omega)$. For simplicity, proofs are often presented for $r = 0$, meaning $L^2(\partial\Omega)$ density in Hilbert spaces, but this may be extended to Sobolev spaces, using duality in Banach spaces (through Fubini's theorem)

$$\begin{aligned}
&\langle \tau_\gamma\mathscr{L}_{\partial\Omega}\alpha, \phi\rangle_{H^s(\gamma)\times H^{-s}(\gamma)}\\
&\quad= \int_\gamma\int_{\partial\Omega} \Phi(x-y)\alpha(x)\,dx\phi(y)\,dy\\
&\quad= \int_{\partial\Omega}\alpha(x)\int_\gamma \Phi(x-y)\phi(y)\,dy\,dx\\
&\quad= \langle \alpha, \tau_{\partial\Omega}\mathscr{L}_\gamma\phi\rangle_{H^r(\partial\Omega)\times H^{-r}(\partial\Omega).}
\end{aligned}$$

This theorem allows to recover the admissible source sets defined in previous works (e.g. [1,2]) in a more general situation that also includes open sets ω.

Corollary 3.1. *The following are admissible source sets for density*:

- (A1) *An open set $\omega \subset \mathbb{R}^d\backslash\overline{\Omega}$ with components in each external part.*
- (A2) *A boundary set $\gamma = \partial\omega$ where $\omega \subset \mathbb{R}^d\backslash\overline{\Omega}$ is an open set with components in each external part. In this open set ω the Dirichlet problem is well posed* (*note that if ω is unbounded, the exterior problem must have appropriate asymptotic conditions*; *and in wave problems the choices for ω must exclude eigenfrequencies*).
- (A3) *A part of a boundary set $\gamma \subset \partial\omega$, when $\partial\omega$ is an analytic boundary set verifying* (A2), *and γ is open in the $\partial\omega$ topology*;

Proof. Take $w = \mathscr{L}_{\partial\Omega}\alpha$, which is analytic everywhere except at $\partial\Omega$.

(A1) If $w = 0$ in the open set ω, then by analytic continuation, in each connected component, we have $w = 0$ in $\mathbb{R}^d\backslash\overline{\Omega}$.

(A2) Since the Dirichlet problem is well posed and w verifies the equation on ω with $w = 0$ on $\partial\omega$, this implies $w = 0$ in the open set ω, and again by analytic continuation, we have $w = 0$ in $\mathbb{R}^d\backslash\overline{\Omega}$.

(A3) It follows from (A2) since w is analytic on $\partial\omega$ and $w = 0$ on γ implies $w = 0$ on the analytic $\partial\omega$. □

Remark 3.3. The first case presents no problem for the Laplace operator, but in the case of the Helmholtz operator, a set ω without κ as resonance frequency should be considered.

In the second case, to verify the asymptotic condition, it might be needed to add extra functions. This is the case for the Laplace operator in 2D, where a constant is needed to ensure that

$$w(y) = A\log|y| + O(1) \quad (\text{when } y \to \infty)$$

with

$$A = \int_{\partial\Omega}\alpha(x)\,ds_x = 0.$$

Adding the unit function to the basis, we impose that $A = \langle 1, \alpha\rangle = 0$, and the logarithmic behavior disappears.

The last case (A3) uses analytic continuation (by zero) on an analytic boundary. This imposes a null condition all over the boundary, reducing it to the previous cases.

Although the choices (A1), (A2) or (A3) are possible, for a simple connected Ω, a *surrounding boundary* $\gamma = \partial\omega$ with $\mathbb{R}^d\backslash\overline{\omega} \supset \overline{\Omega}$ is usually adopted since it provides better numerical results (this is a particular form of the second case).

Remark 3.4. The previous remark tells us that source points on a boundary $\gamma = \partial\omega$ are sufficient to ensure density. Therefore, taking more source points inside the domain ω is somehow redundant, and it will increase ill conditioning, while solving the linear system.

In discrete terms it is somehow unimportant to know if the points are taken from a boundary or from an open set. They are just isolated points, and we can define boundaries that go through any finite set of source points chosen from an open set.

3.3. Linear independence

In terms of linear independence, we have the following linear independence result for a finite set of point-sources, which is mainly suited for the discretization.

Theorem 4. *A finite set of external point-sources defined by the centers $y_1, \ldots, y_m \in \mathbb{R}^d \backslash \overline{\Omega}$ is linear independent on the boundary $\partial\Omega$ and therefore in Ω.*

Proof. Assume that $v_m(x) = \sum \Phi(x - y_j)\alpha_j = 0$, for $x \in \partial\Omega$. Then the well posedness of the problem implies $v_m \equiv 0$ in Ω. Therefore, by analytic extension $v_m(x) = 0$ for all $x \in \mathbb{R}^d \backslash \{y_j\}_{j=1}^m$. Moreover, applying the differential operator, $\mathscr{A}v_m = \sum \alpha_j \delta_{y_j}$ is null and the result follows from the linear independence of the Dirac deltas. □

Since density results do not hold for isolated points, we should also check the linear independence of point-sources in continuous terms, in the whole set. For a source set γ, this means

$$\mathrm{Ker}(\tau_{\partial\Omega}\mathscr{L}_\gamma) = \{0\}.$$

The proof is dual to the one presented for the density theorem. The roles are now inverted. Having this null kernel, we then could use a boundary source set $\partial\Omega$ to approximate functions defined on the source set γ. While considering boundary source sets $\gamma = \partial\omega$, the condition

$$\mathrm{Ker}(\tau_{\partial\Omega}\mathscr{L}_{\partial\omega}) = \{0\}$$

is verified if we prove density with source sets $\partial\Omega$ for boundary functions on $\partial\omega$.

We have a Fredholm alternative expressed in terms of linear independence and density.

- The linear independence on $\partial\Omega$ is verified for a source set $\gamma = \partial\omega$ if we have proven density on $\partial\omega$ using $\partial\Omega$ as source sets.

This is the case for the *admissible source sets* (A2) and (A3), but not for (A1). When we consider an open source set ω, the functions defined by the adjoint $\tau_\omega \mathscr{L}_{\partial\Omega}$ verify the homogeneous equation $\mathscr{A}u = 0$ in ω, and it will be impossible to approximate functions that do not verify this equation.

We should say that (A1) is admissible for density but it is not admissible for linear independence.

3.4. Weak form and least squares

When applied to some regular data, the MFS performs better with interpolation ($n = m$) than with least squares ($n \geq m$). However, in more general situations, the least squares approach is more stable, avoiding extra interpolation instabilities that arise from rough data. In this section we relate the least squares approach of the MFS to its Galerkin formulation. The Galerkin approach in terms of single layer potentials has also been presented in the works by Dreyfuss and Rappaz [18,19] without relating it to the MFS least squares approach.

Let Γ be the boundary and $\hat{\Gamma}$ be the admissible artificial boundary. Taking β as test functions, the boundary Galerkin formulation (of the integral equation) on Γ gives (complex case)

$$\langle \mathscr{L}_{\hat{\Gamma}}\alpha, \beta \rangle_\Gamma = \int_\Gamma \int_{\hat{\Gamma}} \Phi_y(x)\alpha(y)\, ds_y \overline{\beta}(x)\, ds_x = \langle g, \beta \rangle_\Gamma.$$

From the density results, we can use point-sources as test functions, i.e. $\beta = \Phi_z$ with $z \in \hat{\Gamma}$. This gives

$$\int_\Gamma \overline{\Phi}_z(x) \int_{\hat{\Gamma}} \Phi_y(x)\alpha(y)\, ds_y\, ds_x = \int_\Gamma \overline{\Phi}_z(x) g(x)\, ds_x.$$

In discrete terms this corresponds to considering

$$\sum_{i=1}^n \overline{\Phi}_{z_k}(x_i) \sum_{j=1}^m \Phi_{y_j}(x_i)\alpha_j = \sum_{i=1}^n \overline{\Phi}_{z_k}(x_i) g_i \quad (\text{with } z_k \in \hat{\Gamma}).$$

By choosing an equal number of source points $z_j = y_j$, this means that we are multiplying both sides of the MFS system $\mathbf{Ma} = \mathbf{g}$ by $\mathbf{M}^*$. Thus, this leads to the least squares approach

$$\mathbf{M}^*\mathbf{Ma} = \mathbf{M}^*\mathbf{g}.$$

This least squares approach avoids interpolation instabilities arising when taking $n = m$ and forcing the boundary condition to hold at some specific points.

In fact, for non-regular data the least squares approach produces usually far better results. Several numerical tests suggest that a good choice in 2D is to take $n = 2m$ (the number of collocation points is double the number of source points). This is partially justified associating the approximation for each pair of collocation points $\{x_n, x_{n+1}\}$ not only to the function values $g_n = g(x_n)$ and $g_{n+1} = g(x_{n+1})$, but also the tangential derivative $\partial g/\partial\tau$ when expressed in terms of a finite difference approximation

$$\frac{\partial g}{\partial \tau}(x_n^*) \approx \frac{g_{n+1} - g_n}{h_n}$$

with $h_n = |x_{n+1} - x_n|$ and $x_n^* \in [x_n, x_{n+1}]_\Gamma \subset \Gamma$ (any point on the boundary arc).

3.5. Ill conditioning vs. accurate results

In the MFS, a new paradigm occurs—ill conditioned systems lead to accurate results. This is also known in RBF approximation, and it has already been called *the uncertainty principle* (cf. [33,34]). This phenomenon can be proved for the MFS, using the special framework of concentric circles, and it can be seen in other geometries.

Concentric circles. Consider the simple case of a circular boundary Γ with unitary radius and an admissible exterior source set $\hat{\Gamma}$ defined by a circle of radius R. Let u_m be the approximation obtained by the MFS (11) of the boundary data g, with m sources and $n = m$ collocation points, uniformly (angular) spaced on the circles. We have an error estimate, in this case of concentric circles (cf. [26,31]—Laplace, cf. [14]—Helmholtz), of the form

$$\|g - u_m\|_{L^2(\Gamma)} \leq CR^{-m} \tag{19}$$

with a constant $C > 0$ not depending on m. This estimate is obtained assuming that the function g is the trace of an entire function (and no machine precision problems occur). This shows the exponential rate of convergence for regular boundary data, if ill conditioning is avoided. A similar estimate can be derived (with a smaller rate $R^{-m/2}$), under weaker restrictions on the analytic extension of g (an annulus containing Γ).

On the other hand, it is possible to prove (under similar assumptions, cf. [27,36]) that the condition number (in the

2-norm) of the MFS matrix $\mathbf{M}$ verifies

$$\mathrm{cond}_2\mathbf{M} = O(mR^{m/2}\log R).$$

Therefore, increasing the number of point-sources, or the circle radius R, gives us not only high accuracy, but also severe ill conditioning. Thus one should consider a pseudo-inverse solution taken with a small Tikhonov regularization parameter τ

$$(\tau\mathbf{I} + \mathbf{M}^*\mathbf{M})\mathbf{a} = \mathbf{M}^*\mathbf{g}.$$

It is clear that we cannot hope to get approximations that are better than the order of perturbation induced by the presence of the Tikhonov parameter, that should be around machine precision infinitesimals, following the Morozov discrepancy principle.

Difficulties with sources placed far away from the boundary. From these results on concentric circles for regular data we could be mislead to think that a good choice is to take source points far from the boundary, and that only presents a problem in terms of ill conditioning. This is not so. It is straightforward to consider analytic data on an analytic boundary that leads to a poor MFS approximation when the source points are far from the boundary.

Suppose that $g(x) = \Phi(x - z)$ with z outside the domain Ω, but near the analytic boundary $\Gamma = \partial\Omega$. Then if we take a source set $\hat{\Gamma} = \partial\hat{\Omega}$ (with $\hat{\Omega} \supset \overline{\Omega}$), the approximation is analytic on the whole $\hat{\Omega}$ and in particular near the singularity $z \in \hat{\Omega}\backslash\overline{\Omega}$. Thus the MFS approximation with source points placed far away must fail near the singularity point z, and most importantly, on the nearby boundary points.

We conclude that, even for analytic boundaries, taking the source points far from the boundary may lead to MFS failure, for some analytic boundary data. To this fact we must add the ill conditioning difficulties.

Difficulties with sources placed near the boundary. On the other hand, while taking point-sources near the boundary we have the opposite situation—better conditioning and worse results. This situation approaches the boundary element method (BEM), as the points get closer to the boundary. However, as the MFS does not take into account the singular integration, the results for this source choice get poorer near the boundary. It is easy to check that we may have almost diagonal dominant matrices in this situation (interpolation case), when the fundamental solution is singular at the origin,

$$|M_{ii}| = |\Phi(x_i - y_i)| \longrightarrow \infty \quad (\text{when } y_i \to x_i)$$

and the collocation points are apart (meaning $|x_i - x_{i\pm1}| \gg |x_i - y_i|$).

Thus, in the limit this may lead to a system of the form $\mathbf{Ma} = (\mathbf{D} + \mathbf{E})\mathbf{a} = \mathbf{g}$ with a high diagonal matrix $\mathbf{D} \approx \zeta\mathbf{I}$ (with large $|\zeta|$) and a smaller residual matrix $\mathbf{E}$. Near the boundary collocation points the solution would behave like $\tilde{u}(x) \approx g(x_i)\Phi(x - x_i)/\zeta$ (for $x \approx x_i$), as $\mathbf{a} \approx \mathbf{g}/\zeta$. This would restrict the approximation to $g(x) \approx g(x_i)\Phi(x - x_i)/\zeta$, which is not true for general g.

We conclude that source points placed near the boundary may improve the conditioning if they are apart, but then this cannot lead to good MFS approximations.

3.6. Normal direction choice for the source points

From the previous considerations we see that we may have problems with source sets placed too far from the boundary and also when they are too close to the boundary (see also [25]).

We recall the *normal direction choice for source points* proposed in [5,6], in the context of eigenvalue calculation.

Step 1: Take collocation points $x_1, \ldots, x_n \in \partial\Omega$ (when possible almost equally spaced).

Step 2: Define the approximate normal vectors (in 2D):

$$\tilde{\mathbf{n}}_i = \tfrac{1}{2}((x_i - x_{i-1})^\perp + (x_{i+1} - x_i)^\perp)$$

with the orthogonal notation $z^\perp = (-z_2, z_1)$, and take

$$y_i = x_i + \beta\tilde{\mathbf{n}}_i$$

with some coefficient β (that may also depend on i).

Again we may leave the coefficient β unprecised. For non-convex domains a larger β may lead to intersections that might be avoided taking different β values for each i. Anyhow, taking a constant $\beta = 1$ is a non-optimal choice that works in most cases.

If we want better results for regular data, we may take larger β. This normal direction choice for source points has been extensively used for eigenvalue calculation, being the only one found to be robust to the interpolation case. This choice for the eigenvalue problem may be improved for boundary problems, as the function is not meant to be constant along the boundary. This lead to the notion of *glocal choice* for β recently presented in [4].

Glocal choice for the source set: The MFS is a global method where the approximation in one part of the boundary affects the rest. To circumvent this problem and without complicating too much the MFS—that should be preserved simple—we propose to choose the parameter β using the local information of the function g (this lead to the name *glocal* currently used in the globalization context).

The idea consists in taking a number of boundary points $x_{i-p}, \ldots, x_{i+p}$ and to find the $y_{i-q}, \ldots, y_{i+q}$ (with $p \geq q$) such that

$$y^\beta_{i+j} = x_{i+j} + \beta\tilde{\mathbf{n}}_{i+j} \quad (\text{with } j = -q, \ldots, q)$$

gives the best MFS approximation (in terms of the constant β) for the boundary data vector $\mathbf{g}_i = (g(x_{i-p}), \ldots, g(x_{i+p}))$. It should be noticed that $q > 1$ may lead to an expensive algorithm. We may consider for instance $q = 1$ or 2 and $p = 3$ or 5. In this simple situation we have to solve several $q \times q$ MFS least squares systems

$$(\mathbf{M}^\beta_i)^*\mathbf{M}^\beta_i\mathbf{a}^\beta_i = (\mathbf{M}^\beta_i)^*\mathbf{g}_i \quad (\text{with } \mathbf{M}^\beta_i = [\Phi(x_{i+j_1} - y^\beta_{i+j_2})]_{p\times q})$$

and choose along a discrete number of β the one that minimizes the residual $\mathrm{Res}(\beta) = \|\mathbf{M}^\beta_i\mathbf{a}^\beta_i - \mathbf{g}_i\|$.

- The advantage of this *glocal* technique is to adapt the location of the point-sources to fit locally the boundary data. Only afterwards we use the chosen source points to perform the global approximation.
- The main disadvantage of this technique is that it is a bit expensive for the preliminary source points calculation and is not consistent with the simplicity of the MFS. In several experiments carried out for the Laplace equation the improvement gained with this glocal β choice does not compensate with respect to the simpler constant β choice. Improvements were more significant with Helmholtz numerical tests, but this is beyond the scope of this study.

4. Some extensions of the MFS

As a consequence of the density results it is clear that sometimes the point-sources may be not enough to perform the MFS approximation. For instance in the simple case of the 2D Laplace equation we need to include a constant as an extra function. It should be noted that this may still be viewed in the context of fundamental solutions, as the constant verifies the Laplace equation.

In fact, we may consider the extended MFS approximation to be written as

$$\tilde{u}(x) = \alpha_1\Phi(x - y_1) + \cdots + \alpha_m\Phi(x - y_m) + \alpha_0(\Phi(x - y_1) - 1)$$

noting that $\phi(x-y_1)=\Phi(x-y_1)-1$ is also a point-source for the different fundamental solution $\phi(x)=\Phi(x)-1$ of the Laplace equation.

Moreover, this approximation is exactly the same but written with the constant term

$$\tilde{u}(x)=\beta_0+\beta_1\Phi(x-y_1)+\cdots+\beta_m\Phi(x-y_m)$$

by taking $\beta_0=-\alpha_0,\beta_1=\alpha_0+\alpha_1$, and all the remaining terms equal ($k\geq 2$), $\beta_k=\alpha_k$.

Thus we should not only restrict the MFS to the usual choice of the fundamental solution.

Some enrichments of the MFS space of basis functions may still be viewed in the context of fundamental solutions.

In particular these enrichments include all the entire functions (functions that verify the equation in the whole space):

(i) For instance, we may include harmonic polynomials P_k in the context of Laplace fundamental solutions by adding a single external source point y:

$$\tilde{u}(x)=\alpha_0\Phi(x-y)+\alpha_1(\Phi(x-y)+P_1(x))+\cdots+\alpha_m(\Phi(x-y)+P_m(x))$$

as each $\phi_k(x-y)=\Phi(x-y)+P_k(x)$ is a point-source centered at y.

(ii) In a similar fashion, we may include plane waves $W(x)=e^{i\kappa x\cdot d}$ (with $|d|=1$) in the context of Helmholtz fundamental solutions by adding them to external source points:

$$\tilde{u}(x)=\alpha_1\Phi(x-y_1)+\beta_1(\Phi(x-y_1)-e^{i\kappa x\cdot d_1})+\cdots+\alpha_m\Phi(x-y_m)+\beta_m(\Phi(x-y_m)-e^{i\kappa x\cdot d_m})$$

as each $\phi_j(x-y_j)=\Phi(x-y_j)+e^{i\kappa x\cdot d_m}$ is a point-source centered at y_j. It is clear that by adding the plane waves we loose the correct asymptotic behavior given by the Sommerfeld radiation condition, but this will work as well for interior boundary problems.

Therefore, we stress that some enrichments of the MFS may still be viewed as MFS methods if we are not restricted to using only the conventional fundamental solution for each equation.

We recall that enrichment of the MFS with particular solutions, adapted to some geometrical difficulties—such as cracks—as proposed in [8] may lead to far better results than to remain with the conventional MFS approach. Another possibility is to combine the MFS with other numerical methods such as BEM (e.g. [12]).

In this context we recall other extensions in the next subsections. The asymptotic behavior of the fundamental solutions leads to similar and apparently non-related Trefftz methods, such as the plane waves method, in the context of wave propagation (Section 4.1).

Furthermore, the use of fundamental solutions of the associated eigenvalue equation leads to methods for solving non-homogeneous problems, as presented in [7] (Section 4.2).

Remarkably, we note that by considering the MFS in a higher dimension for standard PDEs, we get the usual RBF approximations, such as MQ, IMQ or Gaussian, as announced in [3] (Section 4.3).

4.1. Asymptotic MFS

As stated in the previous section, under some assumptions the MFS performs with an exponential rate of convergence, placing the source points on a circle with increasing radius. This also suggests that by taking the asymptotic behavior of the fundamental solution, one should obtain similar results. This was shown in [10] for the 2D Helmholtz fundamental solution, establishing a direct connection between this asymptotic MFS and the *plane waves method* (also a Trefftz type method). We recall formula (3), with the behavior of the scattering waves in 3D, in terms of the far field amplitude $u_\infty(\hat{x})$, with $\hat{x}=x/|x|$,

$$u(x)=\frac{e^{i\kappa|x|}}{|x|}(u_\infty(\hat{x})+O(|x|^{-1}))\quad\text{when } |x|\to\infty.$$

For a single layer potential, defined on the boundary $\Gamma=\partial\Omega$,

$$u(x)=\int_\Gamma\frac{e^{ik|x-y|}}{4\pi|x-y|}\alpha(y)\,ds_y$$

the asymptotic behavior of the Helmholtz fundamental solution leads to the far field expression (e.g. [17])

$$u_\infty(\hat{x})=\frac{1}{4\pi}\int_\Gamma e^{-ik\hat{x}\cdot y}\alpha(y)\,ds_y.$$

In a dual fashion, by taking an admissible artificial boundary $\hat{\Gamma}$, it can be shown that the MFS single layer based approximation

$$u(x)=\int_{\hat{\Gamma}}\frac{e^{ik|x-y|}}{4\pi|x-y|}\alpha(y)\,ds_y$$

can be substituted by a Herglotz, superposition of waves approximation (e.g. [17]), using only the plane waves directions $\hat{y}\in S$ (here S stands for the sphere)

$$u(x)=\int_S e^{-ik x\cdot\hat{y}}\alpha(\hat{y})\,d\hat{y}$$

again with density results, that allow this approximation on the boundary Γ.

In the numerical experiments presented in [10] it was clear that this asymptotic MFS performed better, for regular data (assumptions for exponential rate of convergence). It does not avoid ill conditioning, but avoids machine precision problems, by not using a large radius for the enclosing circle. On the other hand, the *plane waves method* is not a suitable method for non-smooth data or for non-simply connected shapes, and of course it cannot be used for exterior problems, since the Sommerfeld radiation condition (3) will not be verified.

4.2. Domain MFS

One of the restrictions of the classical MFS is that it should be applied to homogeneous problems (with $f=0$). A common meshfree approach to deal with non-homogeneous problems is to consider RBF approximations, as in [22,29], to obtain a particular solution of the non-homogeneous part. To stay within the framework of fundamental solutions, the idea of using other fundamental solutions, associated with the eigenvalue equation for the operator $\mathscr{A}$, was introduced in [7].

If Φ_λ is the fundamental solution of $\mathscr{A}-\lambda$ the particular solution can be approximated using density results (on the domain) by

$$u_p(x)=\sum_{k=1}^{p}\sum_{j=1}^{n}\alpha_{jk}\Phi_{\lambda_k}(x-y_j),\tag{20}$$

where the λ_k are chosen values in an interval. In fact, for collocation points x_k inside the domain, and external source points y_j, we get the system of equations

$$f(x_k)=\mathscr{A}u_p(x_k)=\sum_{k=1}^{p}\sum_{j=1}^{n}\lambda_k\alpha_{jk}\Phi_{\lambda_k}(x_k-y_j)\tag{21}$$

and the coefficients α_{jk} for the particular solution u_p can be easily deduced from the coefficients $\beta_{jk}=\lambda_k\alpha_{jk}$, obtained for f. This domain approach of the MFS, is justified by the following density result. For $\mathscr{A}=-\Delta$ (or for $\mathscr{A}=-(\Delta+\kappa^2)$), and Φ_λ being the fundamental solution to the Helmholtz equation, $(\Delta-\lambda)\Phi_\lambda=-\delta$, we have

Theorem 5. *Let $\hat{\Gamma}$ be an admissible source set* (A1, A2 *or* A3) *and I an interval in* $]-\infty,0]$. *The space*

$$\mathbf{S}_{\hat{\Gamma},I,\Omega}=\text{span}\{\Phi_\lambda(x-y)|_\Omega : y\in\hat{\Gamma},\lambda\in I\}$$

is dense in $L^2(\Omega)$.

Proof. See [7]. □

In this approach, we added a frequency dimension, as a way to produce an MFS that allows not only a boundary approximation, but also a domain approximation, and this choice gives a simple form for particular solutions. Another possibility is to use plane waves [10], instead of fundamental solutions, with similar density results, and also with no major restriction in the choice of frequencies λ_k (they do not need to be integers, or to be related to any of the eigenfrequencies of the domain problem).

As we will see in the next subsection, it is possible to establish a direct connection between the most common RBF approximations and the approximation of the MFS in a higher dimension. Therefore, the RBF approach is just another way to add a dimension. In this case a space dimension, that also allows domain approximation (and it has been extensively used in applications).

4.3. RBFs as MFS approximations in a higher dimension

Since most common scalar fundamental solutions have a radial feature, the MFS has been associated with RBFs, as a particular case, when the functions are not singular and have radial properties, for instance thin plate splines. In [3] a missing counterpart was suggested—some of the most common RBF approximation methods are just particular cases of MFS boundary approximations when applied to a higher dimension. In this paragraph we will consider the relation between the MFS boundary interpolation in dimension $d+1$ and the RBF domain interpolation in dimension d, for the most commonly used RBFs.

We shall adopt the following notation: capital bold letters, like $\mathbf{X}=(x_1,x_2,x_3)$ denote a point in 3D that we associate to a lowercase bold letter $\mathbf{x}=(x_1,x_2)\mapsto(x_1,x_2,0)$ representing a 2D point, that is considered to be in the plane $x_3=0$. Likewise, a function value defined in 3D variables will denoted by capital letter like $F(\mathbf{X})$ and its restriction to the plane $x_3=0$, will be denoted simply by $f(\mathbf{x})$, being $f(x_1,x_2)=F(x_1,x_2,0)$.

4.3.1. RBF-MQ in 2D as the MFS for the 3D bilaplacian

Consider a function f, defined in a bounded set $\omega\subset\mathbb{R}^2$, the standard 2D RBF-MQ collocation approach with multiquadrics uses parameters c_j

$$f_N(\mathbf{x})=\sum_{j=1}^{N}a_j\sqrt{|\mathbf{x}-\mathbf{y}^{(j)}|^2+c_j^2}$$

or more precisely, using the notation $\mathbf{x}=(x_1,x_2)$ and $\mathbf{y}_j=(y_1^{(j)},y_2^{(j)})$,

$$f_N(x_1,x_2)=\sum_{j=1}^{N}a_j\sqrt{(x_1-y_1^{(j)})^2+(x_2-y_2^{(j)})^2+c_j^2}.$$

Note that if Δ is the Laplace differential operator in dimension d, we have for $0\neq\mathbf{X}\in\mathbb{R}^d$,

$$\Delta(|\mathbf{X}|^p)=p(d+p-2)|\mathbf{X}|^{p-2}.$$

The fundamental solution (5) verifies $-\Delta(|\mathbf{X}|^{-1})=4\pi\delta$, and therefore from $\Delta^2(|\mathbf{X}|)=\Delta(\Delta(|\mathbf{X}|))=\Delta(2|\mathbf{X}|^{-1})=-8\pi\delta$, a fundamental solution of the bilaplacian in 3D is given by

$$\Phi_{\Delta\Delta}(\mathbf{X})=\frac{-1}{8\pi}|\mathbf{X}|.$$

Now consider the following MFS bilaplacian 3D framework for the boundary approximation:

(i) Boundary points $\mathbf{X}^{(i)}=(\mathbf{x}^{(i)},0)=(x_1^{(i)},x_2^{(i)},0)\in\omega\times\{0\}=\Gamma_\omega\subset\mathbb{R}^3$.
(ii) Source points $\mathbf{Y}^{(j)}=(y_1^{(j)},y_2^{(j)},c_j)\in\hat{\Gamma}_\omega\subset\mathbb{R}^3$.

Considering a discrete set of 3D source points $\mathbf{Y}^{(j)}=(x_1^{(j)},x_2^{(j)},c_j)$, and fitting the coefficients a_j by collocation, we easily get the MFS form in 3D of the RBF-MQ approximation in 2D

$$f_N(\mathbf{x})=-8\pi\sum_{j=1}^{N}a_j\Phi_{\Delta\Delta}(\mathbf{X}-\mathbf{Y}^{(j)}).$$

This immediately relates the RBF-MQ approximation in the 2D domain ω with constant parameters $c_j=c$ to part of the MFS boundary approximation for the 3D bilaplacian using a parallel artificial boundary $\hat{\Gamma}_\omega=\omega\times\{c\}$. This is just a special case of the MFS admissible source sets (A3) where the true boundary is $\Gamma\supset\Gamma_\omega$ and the artificial boundary is $\hat{\Gamma}\supset\hat{\Gamma}_\omega$. It should be mentioned that in this case single and double layer potentials should be both included to ensure density, because we are considering the fundamental solution of a fourth order differential operator.

4.3.2. RBF-IMQ in 2D as the MFS for the 3D Laplacian

Using inverse multiquadrics (IMQ), the 2D RBF-IMQ collocation approach leads to

$$f_N(\mathbf{x})=\sum_{j=1}^{N}\frac{b_j}{\sqrt{|\mathbf{x}-\mathbf{y}^{(j)}|^2+c_j^2}}.$$

Considering Φ_Δ to be the fundamental solution of Laplacian (5) in 3D, with the same MFS 3D framework (i) + (ii), and considering the same source points $\mathbf{Y}^{(j)}$, we get the MFS form of the RBF-IMQ approximation

$$f_N(\mathbf{x})=4\pi\sum_{j=1}^{N}a_j\Phi_\Delta(\mathbf{X}-\mathbf{Y}^{(j)}).$$

Remark. (i) The source set $\hat{\Gamma}_\omega$ is only a particular case for possible admissible source sets. In this case, for constant $c_j=c$, the source set is included in a plane, $\hat{\Gamma}_\omega\subset\mathbb{R}^2\times\{c\}$, and the (A3) condition for admissible source sets is verified when we have the well posedness of the half space problem.

(ii) As stated in [3], other connections can be established. For instance, the extra dimension could be time or frequency. In time, Gaussian RBF are related to the MFS for the heat equation. In frequency, new Helmholtz RBFs can be derived from the MFS (cf. [7]), and can be related to the PDE Kansa type RBF method (cf. [24]), as suggested in [11].

5. Numerical illustrations

In this numerical section we present some simulations that illustrate some of the statements made in the previous sections. The list of numerical experiments to illustrate all the previous considerations would be too long and we selected some experiments that are perhaps less obvious (Section 5.1) or more important (Section 5.2) for the choice of source points in the MFS. We considered the usual Dirichlet problem for the 2D Laplace problem.

5.1. Unusual source set configurations

In this first simulation we consider a domain Ω_1 with a boundary parametrized, in the complex Argand plane, by

$$\partial\Omega_1 : t \in [0, 2\pi[\mapsto (2 + \tfrac{1}{10}\sin(4t))e^{it}$$

and in this boundary we considered $n = 60$ collocation points, see Fig. 1 (blue dots). As a test we considered also $m = 60$ source points distributed on a vertical line:

(*Source set* 1) The first source line L_a is given by $t \mapsto 1 + it$, and it crosses the domain. We took source points in two segments, with $|t| \in [3, 5]$, both outside the domain. This is a non-admissible situation.

(*Source set* 2) The second source line L_b is given by $t \mapsto 3 + it$, and it does not cross the domain. Again, take the source points in two segments, with $|t| \in [3, 5]$. This is an admissible situation.

In both cases, we aimed to approximate the boundary Dirichlet data for the Laplace equation:

$$g_1(x) = x_1(x_2 + 1)$$

and the difference between the two simulations is quite clear in Figs. 1 and 2. When the line L_a crosses the domain (see Fig. 1(a)), it is not possible to approximate this data, and the MFS basically returns noise (Fig. 1(b)). On the other hand, when the line L_b does not cross the domain (see Fig. 2(a)) the approximation is quite reasonable, and it is even difficult (without a zoom) to distinguish the approximation from the true data (Fig. 2b), and therefore we also present an error plot in Fig. 2(c), using $3n = 180$ test nodes on the boundary.

5.2. The normal direction algorithm for source sets

In this paragraph we present results for a domain given by a conformal mapping of the unitary circle through

$$f(z) = \frac{3z}{2z-4} + \frac{1 - z/4}{2z+3},$$

i.e. $\partial\Omega_2 = f(\partial B(0, 1))$. We also considered simple Dirichlet data given by $g_2(x) = 3 + x_1 + x_2^2$ placed at 120 collocation points (resulting from the f transformation of equally spaced points on the circle). These boundary points (in blue) are presented in Fig. 3(a) and the graph of g_2 in those points is given in Fig. 3(b). In the next figures the source points will be presented as red dots.

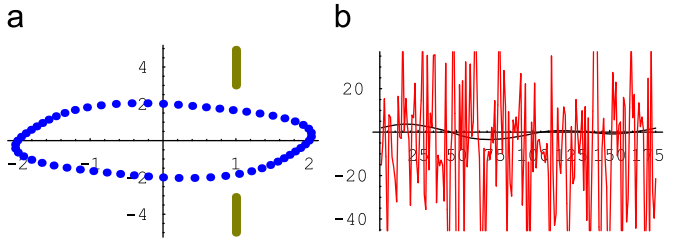

Fig. 1. Source set 1: (a) position of the collocation (blue dots) and source (green dots) points, cutting the domain; (b) poor noisy approximation, corresponding to an impossible approximation. (For interpretation of the references to color in this figure legend, the reader is referred to the web version of this article.)

In the following experiments (Figs. 4–7), we considered 120 uniformly spaced collocation points on $\Gamma = \partial\Omega_2$ and the same number of source points on four different type of source sets $\hat{\Gamma}$: (i) circular, (ii) boundary dilation, (iii) normal direction, (iv) conformal mapping.

Considering a changing parameter μ, we have plotted, in the labeled (a) figures, the evolution of the results in terms of

- the *accuracy* (meaning $-\log_{10}$(error)) and
- the *condition number* (meaning $\log_{10}$(|max /min(eigenvalues)|)).

For the best parameter μ, in each case, we plotted the corresponding source points in the labeled (b) figures, and either the approximation or the error plot in the labeled (c) figures. The approximation/error is plotted with a larger number of test points($3n = 360$ points), as part of step (III) in the MFS algorithm.

5.2.1. Circular source sets

In this case we considered the changing parameter to be the radius, and took $\hat{\Gamma} = \partial B(0, \mu)$. The numerical results for these circular source sets are presented in Fig. 4. In terms of the aforementioned accuracy-conditioning plot, in Fig. 4(a), we see that the results were quite poor (small accuracy, always large condition numbers). The best circular source set was obtained with a radius $\mu = 6.575$ and presented in Fig. 4(b). The maximum error for this best choice was about 0.17, and we see it in Fig. 4(c) the unstable noisy approximation to g_2 (with exact plot in Fig. 3(b)).

5.2.2. Dilation source sets

In this case we considered the changing parameter to be a dilation factor of the original boundary, with $\hat{\Gamma} = (1 + \mu)\Gamma$.

The results for the accuracy-conditioning plot, in Fig. 5(a), were similar, and again quite poor. The best dilation source set was obtained with $\mu = 6.875$ in Fig. 5(b). The maximum error for this best choice was about 0.20 and we see again in Fig. 5(c) an unstable noisy approximation to g_2.

5.2.3. Normal direction algorithm for source points

In this case we considered $\mu = \beta$ in the normal direction algorithm, as explained in Section 3.6.

The accuracy-conditioning plot in Fig. 6(a) shows very good numerical results. The evolution of the results is quite stable and we are able to achieve high accuracy with considerably smaller condition numbers. The best numerical results were obtained

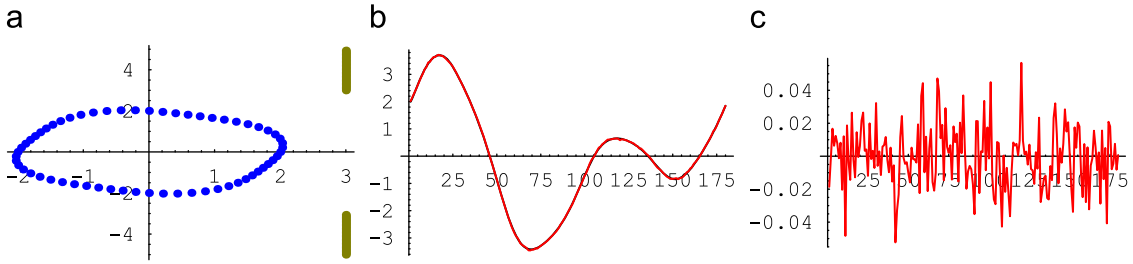

Fig. 2. Source set 2: (a) position of the collocation (blue dots) and source (green dots) points, not cutting the domain; (b) almost coincident results, corresponding to a possible and good approximation; (c) boundary error plot. (For interpretation of the references to color in this figure legend, the reader is referred to the web version of this article.)

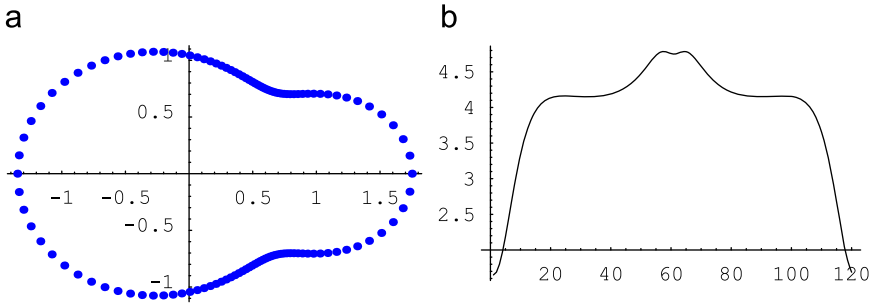

Fig. 3. (a) Collocation points on $\partial\Omega_2$; (b) graph of g_2 on those 120 collocation points.

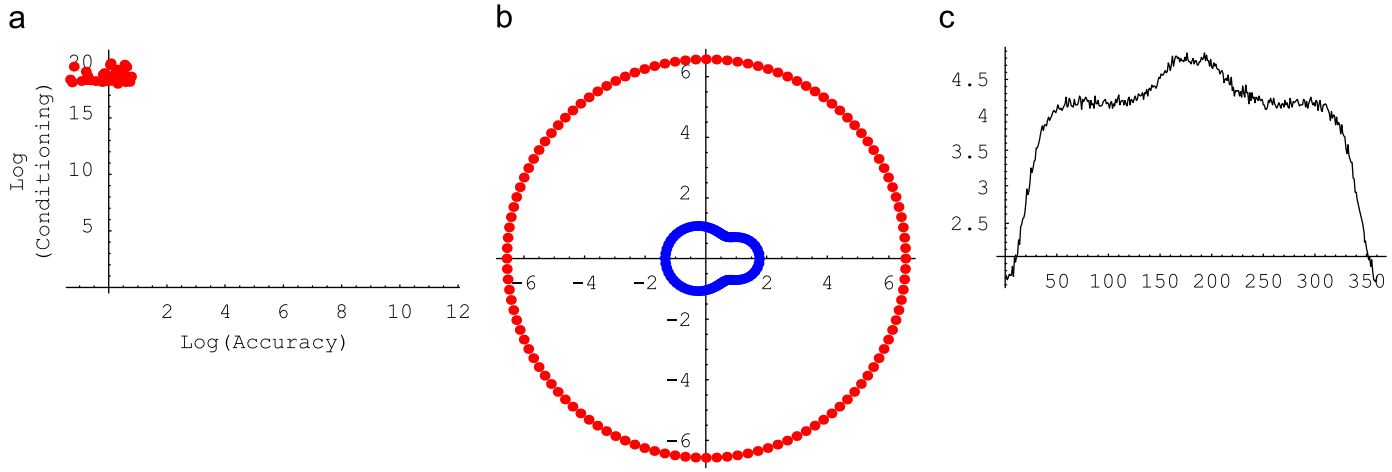

Fig. 4. Circular source sets (i): (a) log–log plot with accuracy vs. conditioning (changing the radius $\mu \in [1.7, 10[_{step=0.125}$); (b) best circular source set (at $\mu = 6.575$), for the given data; (c) approximation of g_2 using (b).

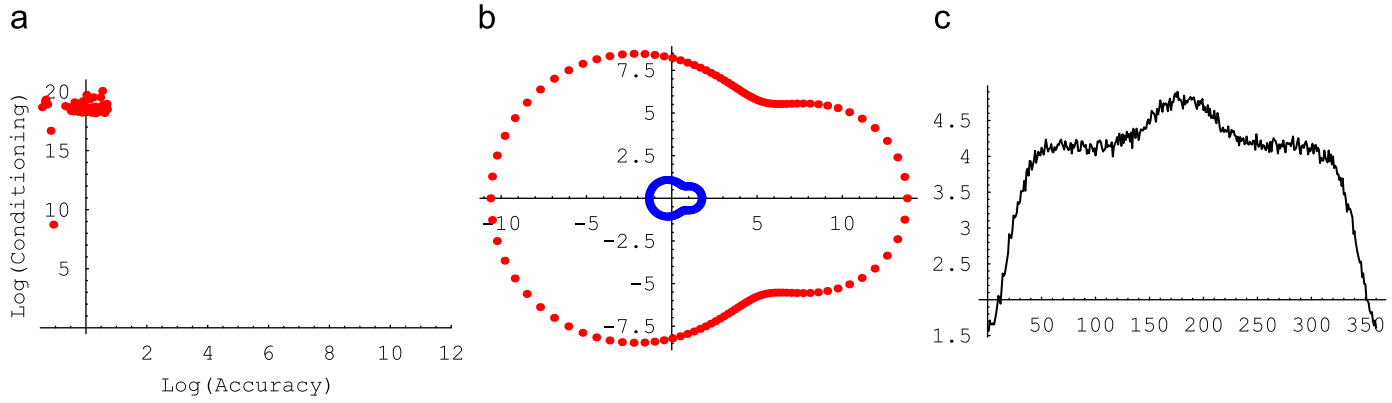

Fig. 5. Dilation source sets (ii): (a) log–log plot with accuracy vs. conditioning (changing the dilation factor $(1+\mu) \in [1, 9]_{step=0.125}$); (b) best dilation source set (at $1+\mu = 7.875$), for the given data; (c) approximation of g_2 using (b).

with $\beta = 4.25$, for the source points presented in Fig. 6(b). The error is plotted in Fig. 6(c)—the maximum error was about 3.6×10^{-9} with a corresponding condition number of 5.3×10^{7}.

5.2.4. *Conformal mapping source sets*

These sets are defined by the transform $f(\partial B(0,\mu))$ with $\mu > 1$ using 120 uniformly spaced points on $\partial B(0,\mu)$.

As the true boundary results from the same conformal map (with $\mu = 1$), this lead to even better numerical results for this simple g_2, as presented in Fig. 6. The accuracy-conditioning plot in Fig. 7(a) leads to a "7 shaped curve", observed for circular domains. We start by poor results with small condition numbers and when arriving to the highest accuracy (almost at machine precision), the higher condition numbers do not improve the results further on, due to machine precision limitations. At the highest condition numbers we may have almost randomly good or bad results. The best conformal mapped source set, with $\mu = 1.45$, is presented in Fig. 7(b) and it is not easily predictable from the original boundary set. In Fig. 7(c) we see the error plot for that best result, with a maximum error about 4.1×10^{-12}, and with condition number about 1.7×10^{11}.

Comments: We could have presented results for other simple and regular g. For some other choices the normal direction algorithm performs better than using conformal mapping source sets (whereas the conformal transform may map the points to

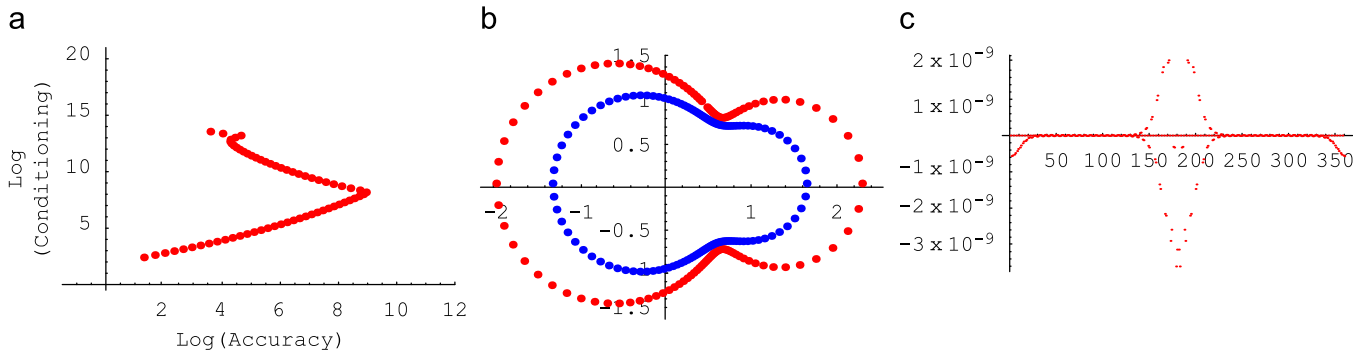

Fig. 6. Normal direction source sets (iii): (a) log–log plot with accuracy vs. conditioning (changing the distance factor $\mu \in]0,8]_{step=0.125}$); (b) best normal direction source set (at $\mu = 4.25$), for the given data; (c) approximation error of g_2 using (b).

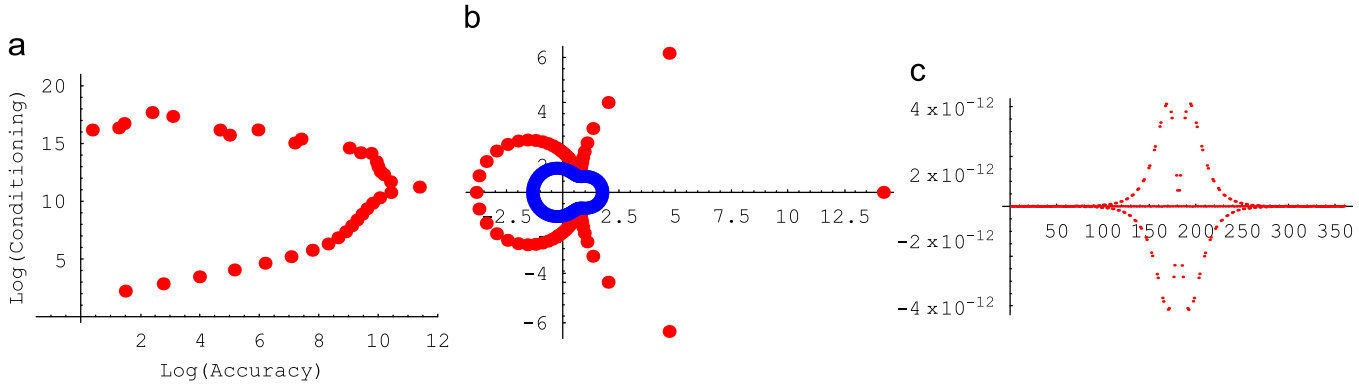

Fig. 7. Conformal mapping source sets (iv): (a) log–$\log_{10}$ plot with accuracy vs. conditioning (changing the mapping circle radius $\mu \in]1,2]_{step=0.025}$); (b) best conformal mapping source set (at $\mu = 1.45$), for the given data; (c) approximation error of g_2 using (b).

unpredictable places). It is more important to stress that unlike the conformal mapping technique that only works in rather simple situations (like this one), the normal direction algorithm is general (it has been tested for other PDEs), simple, reliable and it presents results that may match the highest performance of the MFS.

Acknowledgments

The author acknowledges the financial support from CEMAT and Fundação para a Ciência e Tecnologia (FCT), through projects POCI MAT/61792/2004 and MAT/60863/2004 that enabled him to perform some of this work.

References

[1] Alves CJS. Inverse scattering with spherical incident waves. In: DeSanto J, editor. Mathematical and numerical aspects of wave propagation. Philadelphia, PA: SIAM; 1998. p. 502–4.
[2] Alves CJS. Density results for the Helmholtz equation and the method of fundamental solutions. In: Atluri SN, Brust FW, editors. Advances in computational engineering & sciences, vol. I. Tech Sc. Press; 2000. p. 45–50.
[3] Alves CJS. Preface to the special issue on meshless methods. Eng Anal Boundary Elem 2008;32(6):439.
[4] Alves CJS. Enrichment techniques and the method of fundamental solutions. In: Bergen B, et al. editors. Proceedings of LSAME'08 Leuven symposium on applied mechanical engineering in CD-ROM, 2008.
[5] Alves CJS, Antunes PRS. The method of fundamental solutions applied to the calculation of eigenfrequencies and eigenmodes of 2D simply connected shapes. Comput Mater Continua 2005;2(4):251–66.
[6] Alves CJS, Antunes PRS. The method of fundamental solutions applied to the calculation of eigensolutions for 2D plates. Int J Numer Methods Eng 2009;77:177–94.
[7] Alves CJS, Chen CS. A new method of fundamental solutions applied to nonhomogeneous elliptic problems. Adv Comput Math 2005;23:125–42.
[8] Alves CJS, Leitão VMA. Crack analysis using an enriched MFS domain decomposition technique. Eng Anal Boundary Elem 2006;30(3):160–6.
[9] Alves CJS, Silvestre AL. Density results using Stokeslets and a method of fundamental solutions for the Stokes equations. Eng Anal Boundary Elem 2004;28:1245–52.
[10] Alves CJS, Valtchev SS. Numerical comparison of two meshfree methods for acoustic wave scattering. Eng Anal Boundary Elem 2005;29(4):371–82.
[11] Alves CJS, Valtchev SS. A Kansa type method using fundamental solutions applied to elliptic PDEs. In: Leitão VMA, editor. Advances in meshfree techniques. New York: Springer; 2007. p. 241–56.
[12] Antonio J, Tadeu A, Godinho L. A three-dimensional acoustics model using the method of fundamental solutions. Eng Anal Boundary Elem 2008;32(6):525–31.
[13] Arantes e Oliveira ER. Plane stress analysis by a general integral method. Proc ASCE Eng Mech Division 1968;94:79–101.
[14] Barnett AH, Betcke T. Stability and convergence of the method of fundamental solutions for Helmholtz problems on analytic domains. J Comput Phys 2008;227(14):7003–26.
[15] Bogomolny A. Fundamental solutions method for elliptic boundary value problems. SIAM J Numer Anal 1985;22:644–69.
[16] Chen G, Zhou J. Boundary element methods. London: Academic Press; 1992.
[17] Colton D, Kress R. Inverse acoustic and electromagnetic scattering theory, 2nd ed. Berlin, New York: Springer; 1998.
[18] Dreyfuss P, Rappaz J. Numerical analysis of a non-singular boundary integral method. I. The circular case. Math Methods Appl Sci 2001;24:847–63.
[19] Dreyfuss P, Rappaz J. Numerical analysis of a non-singular boundary integral method. II. The general case. Math Methods Appl Sci 2002;25:557–70.
[20] Fairweather G, Karageorghis A. The method of fundamental solutions for elliptic boundary value problems. Adv Comput Math 1998;9:69–95.
[21] Fairweather G, Karageorghis A, Martin P. The method of fundamental solutions for scattering and radiation problems. Eng Anal Boundary Elem 2003;27:759–69.
[22] Golberg MA, Chen CS. The method of fundamental solutions for potential, Helmholtz and diffusion problems. In: Golberg MA, editor. Boundary integral methods and mathematical aspects. Computational Engineering, vol. 1. WIT Press; 1999. p. 103–76.
[23] Hörmander L. Linear partial differential operators. In: Grundelehren der wissenschaften, vol. 119. Berlin: Springer; 1969.

[24] Kansa EJ. Multiquadrics—a scattered data approximation with applications to computational fluid dynamics. Comput Math Appl 1990;19:127–45.
[25] Karageorghis A, Fairweather G. The method of fundamental solutions for the solution of nonlinear plane potential problems. IMA J Numer Anal 1989;9(2):231–42.
[26] Katsurada M. A mathematical study of the charge simulation method. II. J Fac Sci Univ Tokyo Sect 1A Math 1989;36(1):135–62.
[27] Kitagawa T. On the numerical stability of the method of fundamental solution applied to the Dirichlet problem. Japan J Appl Math 1988;5:123–33.
[28] Kress R. Linear integral equations. In: Applied mathematical sciences, 2nd ed., vol. 82, New York: Springer; 1999.
[29] Li X, Golberg MA. On methods for solving the Dirichlet problem for Poisson's equation. In: Boundary elements XXIV (Sintra, 2002). International series on advances in boundary elements, vol. 13. WIT Press; 2002. p. 87–96.
[30] Kupradze VD, Aleksidze MA. The method of functional equations for the approximate solution of certain boundary value problems. Ž. Vyčisl Mat i Mat Fiz 1964;4:683–15.
[31] Li X. On convergence of the method of fundamental solutions for solving the Dirichlet problem of Poisson's equation. Adv Comput Math 2005;23:265–77.
[32] Mathon R, Johnston RL. The approximate solution of elliptic boundary-value problems by fundamental solutions. SIAM J Numer Anal 1977;14:638–50.
[33] Schaback R. Error estimates and condition numbers for radial basis function interpolation. Adv Comput Math 1995;3:251–64.
[34] Schaback R, Wendland H. Kernel techniques: from machine learning to meshless methods. Acta Numer 2006;15:543–639.
[35] Smyrlis Y-S. Applicability and applications of the method of fundamental solutions. Math Comp 2009;78:1399–1434.
[36] Smyrlis Y-S, Karageorghis A. Some aspects of the method of fundamental solutions for certain harmonic problems. J Sci Comput 2001;16(3):341–71.
[37] Smyrlis Y-S, Karageorghis A. Efficient implementation of the MFS: the three scenarios. J Comput Appl Math 2009;227(1):83–92.